

HIGH POWER OPERATION OF THE POLYPHASE RESONANT CONVERTER MODULATOR SYSTEM FOR THE SPALLATION NEUTRON SOURCE LINEAR ACCELERATOR *

W. A. Reass, S. E. Apgar, D. M. Baca, J. D. Doss, J. M. Gonzales, R. F. Gribble, P. G. Trujillo
Los Alamos National Laboratory, PO Box 1663, Mail Stop H-827
Los Alamos, New Mexico, 87545, U.S.A.

43

Abstract

The Spallation Neutron Source (SNS) is a new 1.4 MW average power beam, 1 GeV accelerator being built at Oak Ridge National Laboratory. The accelerator requires 15 "long-pulse" converter-modulator stations each providing a maximum of 11 MW pulses with a 1.1 MW average power. Two variants of the converter-modulator are utilized, an 80 kV and a 140 kV design, the voltage dependant on the type of klystron load. The converter-modulator can be described as a resonant zero-voltage-switching polyphase boost inverter. As noted in Figure 1, each converter modulator derives its buss voltage from a standard 13.8 kV to 2100 Y (1.5 MVA) substation cast-core transformer. The substation also contains harmonic traps and filters to accommodate IEEE 519 and 141 regulations. Each substation is followed by an SCR pre-regulator to accommodate system voltage changes from no load to full load, in addition to providing a soft-start function. Energy storage and filtering is provided by special low inductance self-clearing metallized hazy polypropylene traction capacitors. Three "H-Bridge" Insulated Gate Bipolar Transistor (IGBT) switching networks are used to generate the polyphase 20 kHz transformer primary drive waveforms. The 20 kHz drive waveforms are chirped the appropriate duration to generate the desired klystron pulse width. PWM (pulse width modulation) of the individual 20 kHz pulses is utilized to provide regulated output waveforms with DSP (digital signal processor) based adaptive feedforward and

feedback techniques. The boost transformer design utilizes amorphous nanocrystalline material that provides the required low core loss at design flux levels and switching frequencies. By resonating the transformer secondary leakage inductance, voltage multiplication and IGBT zero-voltage-switching can be attained. The transformers are wound for leakage inductance, not turns ratio, and a 1:18 turns ratio results in a 1:60 output. The resonant topology has the added benefit of being deQed in a klystron fault (shorted output) condition, with little energy transfer during an arc-down situation. This obviates the need of crowbars and other related protective networks. A review of these design parameters, operational performance at design power levels, and production status will be presented.

I. CONVERTER MODULATOR ASSEMBLY

A view of the completed converter modulator assembly is shown in Figure 2. The oil tank, safety enclosure, and water distribution panel are the prominent features that can be noted in this figure. *Dynapower Corporation* located in Burlington, Vermont won the contract for the build-to-print converter modulator assembly. The first 6 production converter modulator assemblies have been delivered to ORNL in the 2nd quarter of fiscal year 2003.

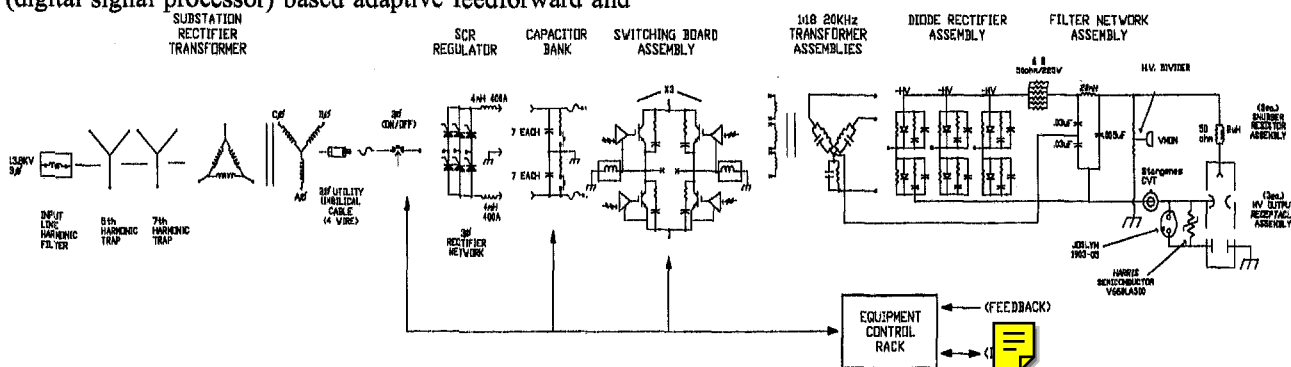


Figure 1. System Block Diagram

* Work supported by the Office of Basic Energy Science, Office of Science of the Department of Energy, and by Oak Ridge National Laboratory.

LOS ALAMOS NATIONAL LABORATORY
3 9338 01006 6735

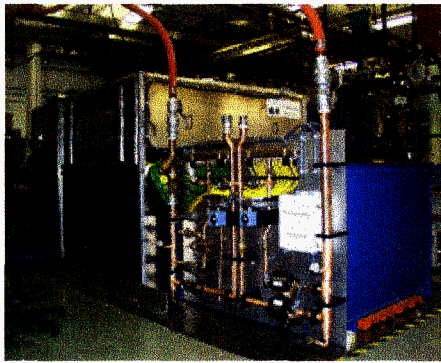


Figure 2. Converter Modulator Assembly

A. Self-Healing Capacitors

Thomson Passive Components (AVX), located in Saint-Apollinaire, France worked with us to develop a lower inductance capacitor for our high power, 20 kHz, switching application. Internal fabrication methodology is optimized to provide enhanced current distribution within the capacitor and also minimize internal interconnect inductance. The all film design provides for excellent energy density and the use of high-ohm metal electrode deposition ensures good current balance through all the internal foil packs. Bank fusing does not seem to reduce physical IGBT failure damage and fusing is not used in the present production design. However, it appears that the fusing can limit “action” in other failure modes and possibly reduce busswork or cabling damage. This is one area we will again examine in future designs.

B. IGBT Switch Plate Assembly

The IGBT switch plate assemblies are designed to be easily removed like a large printed circuit card, such that maintenance and repair can be accommodated off-line. Sliding high-current contacts of multilam louvers interface to the transformer primary busswork, which terminate on the modulator tank lid. Each switch plate contains four IGBT’s in an “H-bridge” configuration. The IGBT device family is the 3300 Volt, 1200 Ampere devices. The *Eupec* FZ1200R33KL2 device is being utilized that have an improved “FIT” rate for higher voltage reliability. The mechanical design of the switch plate assembly has the IGBT’s terminals directly opposite one-another (face-to-face), to provide a low inductance interconnection methodology. This results in a buss-work rail-to-rail inductance (V+ to V-) of ~4 nH. This low inductance is necessary for “snubberless” IGBT switching. Low inductance (~9 nH), high frequency IGBT bypass capacitors for this assembly have been developed by *General Atomics Energy Products* (formerly Maxwell) and are shown in Figure 3. The resulting inductance of the IGBT switch plate network of ~7 nH is desirable to minimize overshoot and ringing from the multi-kA 20 kHz switching that can have dI/dT ’s of ~10 kA/uS. The IGBT switch plate assemblies also must switch the peak power of the system, 11 MW, not just the average power. With the high peak powers involved, additional “on

board” energy storage is provided by 8 each 10 uF, 2 kV capacitors, also manufactured by *General Atomics Energy Products*.

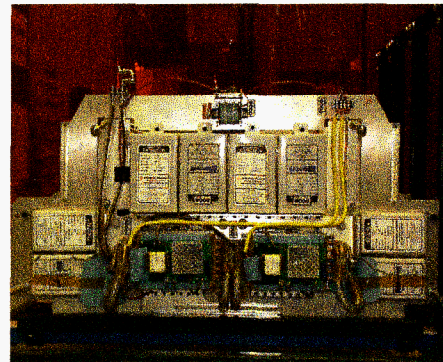


Figure 3. IGBT Switch Plate Assembly

C. Amorphous Nanocrystalline Boost Transformers

The development of the amorphous nanocrystalline transformer core was another long lead development for this project. The characteristics of the nano material are given in Table 1.

Table 1. Nano Material Characteristics

Mu	50,000
Lamination Thickness	.0008"
Stacking Factor	~90%
Bsat	12.3 kG
Core Loss (our use)	~300 W
Core Weight (our use)	~95 lbs
Power (each core)	330 kW

The amorphous nanocrystalline material has exceptional performance as a function of frequency and flux density with the added benefit of having “zero-magnetostriction”. It does not vibrate or make significant noise with excitation. The windings on the core are wound as two single layer solenoids. A view of the nanocrystalline boost transformer is shown in Figure 4. The overall height is about 24" tall with a total assembly weight of ~150 lbs.

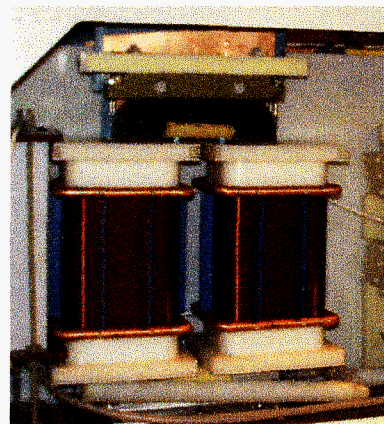


Figure 4. 330 kW Nanocrystalline Boost Transformer

The secondary windings are resonated with tuning capacitors which provide two important functions, (1) an optimized value provides “zero-voltage-switching” for the IGBT’s, and (2), the multiple transformer resonant circuits create “polyphase resonant voltage multiplication”. The transformers are wound with a ratio of 1:19, but the output is about 1:60. Unlike previous power transformers with the same “volts-per-turn” for both the primary and secondary, this design generates multiple volts-per-turn on the secondary. In addition, the core flux expended is that of the primary. It would seem that the secondary leakage inductance isolates the core from the voltage swing generated on the secondary. The zero-voltage-switching characteristic minimizes the IGBT switching loss, turn on is soft without forced commutation (and losses) of the opposite IGBT free-wheeling diode.

D. Resonant Rectification System

To provide six pulse rectification of the 20 kHz, ~140 kV line-line voltages, resonant rectification techniques are used. Capacitors are placed in parallel with groups of rectification diodes. However, low loss; fast recovery diodes are still necessary for this design. 1,600 volt, 70 Amp ion implanted diodes manufactured by IXYS are used in the 140 kV modulator assemblies. The circuit effect of the added rectification capacitance is that it acts like the transformer resonating capacitors and must be considered in the analysis of the transformer tuning. The resonant rectification capacitors have the desirous effect to remove switching transients and “Miller” (ground) capacitance from the diodes. The Miller capacitance (to ground) can cause significant over-voltage of diodes high in the stack. The resonant rectification capacitors effectively swamp this failure mode.

II. COMPONENT AND SYSTEM CHARACTERIZATION

Characterization of the system as related to the component capabilities is very important to optimize performance, reliability, and efficiency. Figure 5 shows the 20 kHz, 3 ϕ transformer drives waveform (2 kV/div and 200uS/div) at full power output. The (136 kV, 9.75 MW) output pulse has the same width as the pulse train, ~1.35 ms.

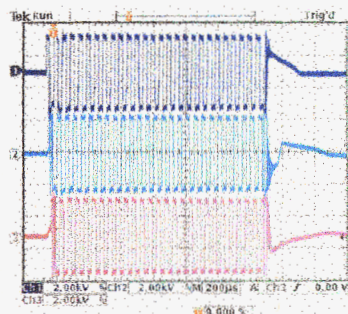


Figure 5. Transformer Drive at Full Power

What can be noted from the drive waveforms are slight oscillations at turn-on related to coupling between phases in association with the truncated start pulses necessary to maintain near-zero core flux offset. The first pulse for each phase has a defined pulse width such that the small nano-cores do not saturate. Additionally, free-wheeling-diode (FWD) recovery properties affect the oscillations and contribute significantly to these oscillations. Although these oscillations do not seem to be detrimental, we are investigating start-up timing methods that maintain zero core flux offset and minimize ringing. We have also evaluated the performance of various IGBT’s in our system. In Figure 6, the upper and middle trace show the Eupec and Mitsubishi IGBT switching characteristics, respectively, at full power with identical gate drive circuits. In our application the Eupec IGBT’s had significantly lower switching losses. However, Mitsubishi does not require a “Cge” and this may have skewed the results of this test.

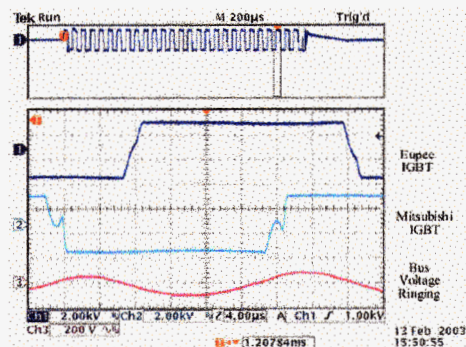


Figure 6. IGBT Switching Performance, $R_{G1}=R_{G2}=1.1 \Omega$, $C_{GE}=0.22 \mu F$

The IGBT’s are also subject to the properties of “dynamic saturation” and tail current at turn-off. It requires ~6uS for this class (3300 V) IGBT’s to reach full saturation, as seen in Figure 7. This saturation delay also affects the required network tuning to appropriately achieve “zero-voltage-switching”. To optimize other performance concerns, totem pole switching occurs during the tail current of the complimentary IGBT. This must occur after the collector has fully recovered. This mechanism does contribute to some additional switching losses.

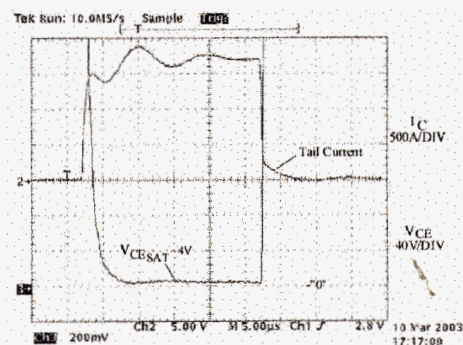


Figure 7. IGBT Dynamic Saturation and Tail Current

III. OPERATIONAL RESULTS AND EFFICIENCY

Operations at full average power were achieved within a week of the installation of the high-power 5MW, 805 MHz Thales klystron. Figure 8 shows the output with 136 kV at the end of the pulse. We have operated the system to the limit of all our present loads, 130 kV at ~450 kW average power with the Marconi 2.5 MW, 402 MHz klystron and ~800 kW average power at 136 kV with the 5MW Thales 805 MHz klystron. With the single 2.5 MW tube, tests interestingly had an electrical efficiency of only ~88%, with ~3.7 kW loss per IGBT. Testing to the full ~136 kV output with the large 5 MW, 805 MHz Thales klystron (~800kW) gave IGBT losses of ~1.7 kW each, with an overall efficiency of 94%. Operation at higher power provides a better match to the resonant converter and affords “zero-voltage-switching” of the IGBTs. Operations continue at the ORNL SNS accelerator. Oak Ridge has operated 24/7 during accelerator RFQ commissioning as well as the recent Drift Tube (DTL) structure commissioning to full power. Start-up problems have been related to vendor Q/A issues and are being worked as the converter-modulator production unfolds.

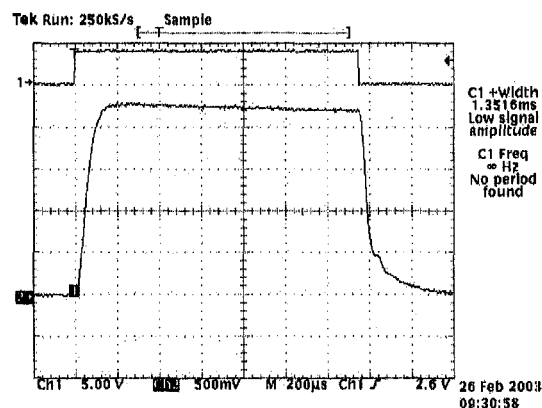


Figure 8. 136 kV Output Pulse

A. Crowbar Tests

Extensive fault testing has also been performed with three times the anticipated SNS high-voltage cable length. These tests have been performed at voltages higher (~145 kV) than anticipated in our operation. Protection of the klystron is not dependant on the inhibit of IGBT switching and IGBT reliability is not dependant on interruption of gate drive during a klystron arc down. Figure 9 shows an arc-down event with the IGBT's continuing to switch, which did not fuse the test wire. In the shorted condition, the resonance of the converter-modulator is deQed, and little power transfer results. The low primary drive voltage coupled into the relatively high leakage inductance of the transformer does not even create an over-current situation for the IGBT's. This provides for a design that has fault “ride-through” capabilities. These results match our modeling.

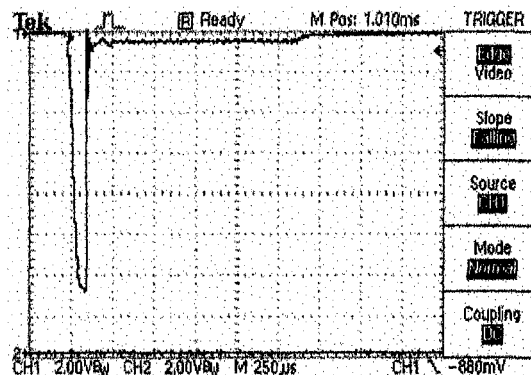


Figure 9. 130 kV Run-On Fault test

IV. SUMMARY

The polyphase resonant converter-modulator has demonstrated several new design methodologies that are expected to revolutionize long-pulse and “CW” modulator designs. These new technologies include special low inductance self-clearing capacitors, large amorphous nanocrystalline cut-core transformers, polyphase resonant voltage multiplication, resonant rectification, snubberless IGBT switching, and adaptive power supply control techniques. Design economies are achieved by the use of industrial traction components such as cast power transformers, IGBT's, and self-clearing capacitors. The compact and modular design minimizes on-site construction and a simplified utility interconnection scheme further reduces installation costs. The design does not require HV capacitor rooms and related crowbars. By generating high-voltage when needed, reliability and personnel safety is greatly enhanced. The system development to date has been completely successful and results indicate that operation to the full system average power (1.1 megawatts) should be achieved as required, within specification, when loads become available.

V. ACKNOWLEDGEMENTS

The authors appreciate the hard work and dedicated efforts of the mechanical and electrical fabrication technicians: Diego C. Jaramillo, Adam R. Martinez, and John J. Sullard.